Article

# The Contrasting Behavior of Strongly and Weakly Interfacially Active Asphaltenes on the Rheology of Model Waxy Oils

Abdulraouf Ali, Ghinwa Yaghy, Laksha Parameswaran, Chris S. Hodges, Thibaut V.J. Charpentier, Simon D. Connell, Kevin J. Roberts, and David Harbottle*

ACCESS | Metrics & More | Article Recommendations | SI Supporting Information

**ABSTRACT:** Asphaltenes and waxes are two components of crude oil that cause flow assurance issues. Although the components coexist, few studies have considered the effect of asphaltenes on wax crystallization and gel-forming properties. Furthermore, the current understanding remains contradictory with both wax-alleviating and wax-aggravating behaviors observed. In this study, asphaltenes extracted from a heavy crude oil were fractionated into strongly and weakly interfacially active asphaltenes by partitioning at a water−oil interface. The two asphaltene fractions exhibited contrasting physicochemical properties, with the strongly interfacially active asphaltenes (IAA) being more polar due to their higher heteroatom content (particularly S and O) and forming larger aggregates in the solution compared to the weakly interfacially active asphaltenes (referred to as remaining asphaltenes, RA). The two asphaltene fractions lowered both the wax gelation temperature and wax appearance temperature; however, the effect was comparable. The unit cell lattice structure of the wax particle remained unchanged in the presence of asphaltenes, but the wax particles were found to be smaller with RA compared to IAA. However, the key finding of the study is how the two asphaltene fractions affected the yield strength of the gelled wax. For RA, the yield strength was lowered with an increasing asphaltene concentration, whereas for IAA, the overall effect was to increase the gel yield strength. Because the properties of the wax particles were largely unchanged by the two asphaltene fractions, the result suggests that the asphaltene−asphaltene interaction contributes to the overall yield strength. It was shown that the interaction between RA and RA is repulsive with negligible adhesion, whereas that between IAA and IAA is attractive with strong adhesion. These structure-breaker and structure-maker properties of the two asphaltenes confirm that the asphaltene−asphaltene interaction significantly contributes to modifying the yield strength of a waxy gel.
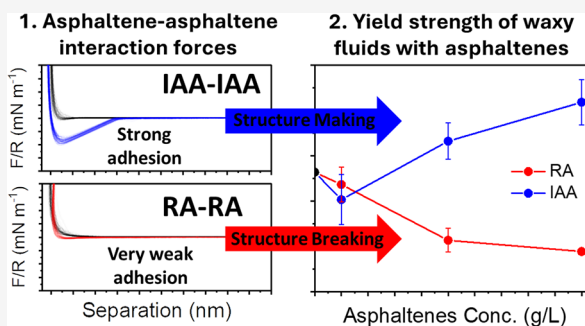
## INTRODUCTION

Crude oil is a mixture of waxes, aromatics, asphaltenes, and resins.[1] Both waxes and asphaltenes have posed significant flow assurance challenges in oil storage, transportation, and processing.[2,3] For waxes, if the fluid temperature drops below the wax appearance temperature (WAT), wax molecules start to interact, crystallize, and form networks, changing the fluid rheology and under some situations causing flow cessation.[4] For asphaltenes, their stability is less sensitive to temperature but is governed by their solvency in crude oil. In poorly solvating environments, asphaltenes have a greater tendency to self-aggregate and form clusters that are sufficiently large that they deposit onto surfaces restricting the flow area.[5−7] Although both fractions contribute to flow assurance issues, it is rare that both fractions are considered together to elucidate how one species affects the other. And given the fact that both waxes and asphaltenes coexist, such knowledge is fundamental to better understanding those flow assurance problems.

Few studies have considered the effects of asphaltenes on wax crystallization and gelation; however, the findings remain contradictory and, therefore, understanding inconclusive. Some studies suggest that asphaltenes cause wax-aggravating effects by enhancing wax nucleation by acting as nucleation sites for wax crystallization, causing the gelation $(T_g)$, wax appearance, and pour point (PP) temperatures to increase.[8,9] Contrastingly, other studies show wax-alleviating effects where the critical temperatures are lowered as a result of inhibiting interactions between wax molecules that is caused by asphaltene molecules sterically hindering the formation of a stable critical nucleus to initiate nucleation.[10−12] And it has
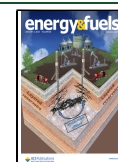
also been discussed that asphaltenes have no effect on the wax crystallization process.[13]

Kriz and Andersen[14] suggested that the wax crystallization and gel strength strongly depend on the concentration and aggregation state of the asphaltenes. When adding dispersed (not extensively flocculated) asphaltenes at concentrations up to 0.01 wt %, the WAT and wax yield stress increased. However, when increasing the asphaltene concentration up to 0.5 wt %, the WAT increased slightly, but the wax yield stress decreased, a behavior attributed by the authors to the increased aggregation state (flocculation) of asphaltenes. Such findings agree with Lei et al.[15] who showed that increasing the amount of aggregated asphaltenes weakened the strength of the waxy network and suppressed $T_g$. For higher asphaltene concentrations, it is generally found that the yield stress,[16−18] WAT,[18,19] and $T_g$[10,18,19] of waxy crude oils decrease, with the mechanism for the changes attributed to the steric hindrance effect previously discussed.[11]

Although most studies consider the effect of whole asphaltenes (WA) on the wax crystallization behavior, recently, others have studied subfractions of WA, with these subfractions exhibiting contrasting physicochemical properties such as polarity. Li et al.[20] and Venkatesan et al.[10] separated asphaltenes of differing polarities based on their relative solubilities in polar (dichloromethane) and nonpolar (pentane) solvents. The more polar fraction was found to be more aromatic and of higher molecular weight compared with the less polar fraction. The less polar asphaltenes reduced the WAT, $T_g$, and yield strength of waxy mixtures more than the polar asphaltenes.[10,20] The authors suggested that the less polar asphaltenes were similar to $n$-paraffins at the molecular level and thus were more able to interact with the waxes. Venkatesan et al.[10] showed that the reduced yield strength in the presence of less polar asphaltenes could be attributed to the changing wax crystal morphology, from needle-like to globular-like crystals that become less entangled and thus do not cause the yield stress to build significantly.

Ruwoldt et al.[19] separated asphaltenes of different polarities using a pseudoextrography method by adsorbing asphaltenes on to calcium carbonate particles. The more polar asphaltenes (termed as "irreversibly adsorbed") had a higher oxygen content (4.48 wt %) and were slightly more aliphatic compared to the least polar fraction (termed as "bulk"). The authors found that the bulk asphaltenes lowered the WAT and yield strength of the waxy fluid, whereas the irreversibly adsorbed fraction had a minimal effect. For the irreversibly adsorbed asphaltenes, the wax crystals were smaller than those formed in the presence of bulk asphaltenes. However, the yield stress reduced only with the bulk asphaltenes, which contradicts the understanding that smaller wax crystals lower the yield stress. The authors suggested that the highly polar asphaltenes acted as "connectors" between wax crystals, commenting that the asphaltenes may be incorporated into the wax crystal via coprecipitation, and the polar moieties of the asphaltenes bridge between the crystals to form an interconnected network of higher strength.

Another method to subfractionate asphaltenes is the so-called extended-SARA method (E-SARA) where WA is separated into strongly and weakly interfacially active asphaltenes by partitioning at an oil−water interface.[6,21,22] These subfractions are commonly termed interfacially active asphaltenes (IAA) and remaining asphaltenes (RA)[23] and have been shown to exhibit differing physicochemical properties.[7,24]

The IAA fraction is more polar, which is attributed to the higher heteroatom content, specifically oxygen, as well as being more multicore and aliphatic compared to the RA fraction. The IAA fraction has a greater tendency to aggregate even in good solvents and forms nanoaggregates and clusters that are larger and more porous than those formed by RA. It is worth noting that the IAA fraction is ∼2 wt % of WA and so is considered to be a minor fraction; however, many flow assurance issues such as deposition and emulsion stabilization are likely caused by this minor but significant fraction.[21,25] And so, the influence of this minor fraction on the properties of waxy fluids warrants further investigation, as to date little is known about how this strongly interfacially active asphaltene behaves in waxy fluids.

For the objective, the effects of the two asphaltene subfractions (RA and IAA) on the bulk properties ($T_g$, WAT, and yield stress) of the waxy model oils have been considered, assessing how differences in the physicochemical properties of the two asphaltene subfractions contribute to modifying the structural and bulk properties of the waxy fluids. A mechanistic model is proposed to describe the observed changes in the waxy fluid yield stress.

## ■ MATERIALS AND METHODS

Asphaltenes were extracted from a Colombian (Llanos region) heavy crude oil with an API of 13.6 (at 60 °F). Further details on the properties of the heavy crude oil have been published by Mojica et al.[26] Whole asphaltenes (WA) were extracted at room temperature by mixing heavy crude oil with $n$-pentane at a ratio of 40:1 (v/v) for 10 min at 15,000 rpm (T18 Ultra-TURRAX, IKA, U.K.). The solution was then left undisturbed for 24 h before filtering (8 $\mu$m Whatman #2 filter paper) under a gentle vacuum. To avoid residual contamination of the asphaltenes by other species, the filter cake was repeatably washed with $n$-pentane until the filtrate ran clear. The washed asphaltenes were then dispersed in toluene (20:1 solvent to asphaltene mass ratio) and centrifuged (Heraeus Megafuge 16 Centrifuge, ThermoFisher Scientific, U.K.) at 10,000 rpm for 40 min to remove any fine mineral solids. The supernatant was removed using a wide-bore pipet and the toluene evaporated to leave the WA sample.

The WA sample was subfractionated into remaining asphaltenes (RA) and interfacially active asphaltenes (IAA) following the method of Ballard et al.[7] and Yang et al.[23] The fractionation method separates asphaltenes based on their interfacial activity at an oil−water interface. In brief, 10 mL of deionized water was homogenized with 100 mL of 10 g/L WA in toluene for 15 min at 24,000 rpm. The stable emulsion was left for 12 h before the supernatant was separated from the emulsion bed. The supernatant was then left in a fume hood to evaporate the solvent and recover the RA fraction. The emulsion bed was gently washed with excess toluene to remove any loosely bound asphaltenes from the water−oil interface before drying the emulsion in a vacuum oven at 60 °C for 12 h to recover the IAA fraction. From 10 g of WA, the amount of IAA extracted was between 0.15 and 0.2 g, meaning that the quantity of IAA in WA is ∼2%. The elemental composition and functional group chemistry of RA and IAA are shown in Table S1 and Figure S1 of the Supporting Information.

**Model Waxy Oils.** A single alkane, $n$-octacosane ($nC_{28}$, melting point of 61−63 °C and >99% purity, Alfa Aesar), was used to prepare the model waxy solutions. Its selection was based on representing the median chain length typically found in paraffinic crude oils.[27] A standard protocol was followed to prepare the test solutions; 4 g of $nC_{28}$ was added to 24 mL of $n$-dodecane (purity of 96% and boiling point of 215 °C, Sigma-Aldrich) and heated at 80 °C for 5 min while gently stirring using a magnetic stirrer. Then, 0.04 g of either asphaltene subfraction, RA or IAA, was added to 16 mL of toluene (purity of ≥99.8% and boiling point of 111 °C, Fisher Scientific) and sonicated for 5 min at ∼80 °C. The high temperature and sonication

were found to be sufficient to disperse the asphaltenes, noting that the IAA fraction is poorly soluble in both good and poor solvents. The asphaltene solution was then poured into the waxy solution at 80 °C, stirred for 5 min, and sonicated for 5 min immediately prior measurement. The test solutions were prepared so that the *n*-dodecane-to-toluene volume ratio was 6:4 (abbreviated as 6:4 DodecTol) and the wax content was 100 g/L. The asphaltene content was varied from 0.1 to 0.5 and to 1 g/L by adjusting the mass of asphaltenes added to toluene. All samples were prepared fresh and used immediately after final sonication to minimize any effects of sample aging.

**Wax Rheology.** Using oscillatory rheology, the wax gelation temperature ($T_g$) was measured at $G' = 1$ Pa (the elastic modulus) as the temperature of the waxy solution was lowered from 35 to 15 °C at 0.5 °C/min. The gelled condition is often defined as $G' = G''$, but for low-viscosity fluids, this is sometimes ambiguous due to instrument inertia, and so $G' = 1$ Pa was taken to be a more reliable criterion.[16] For the measurement, a DHR-2 rheometer (TA Instruments) with a vane (*d*: 15 mm, *l*: 38 mm) and sandblasted cup (*d*: 30.4 mm) were used. Both the geometry and the vane were chosen to minimize any effect of wall slip, and the cup was inserted into the instrument Peltier jacket for temperature control. Instrument calibration followed the standard procedure, and for all measurements, the bearing mode was set to soft. The waxy solution ($V = 40$ mL), with or without asphaltenes, was pipetted into the jacketed cup that was preheated to 80 °C. The solvent trap was added, and the sample was held at temperature for 5 min to achieve thermal equilibrium and for complete dissolution of the wax in the solvent. Then the temperature was lowered to 35 °C by cooling at 10 °C/min before stabilizing for an additional 5 min. The vane was then oscillated at 0.8% strain and 0.5 Hz as the sample temperature was reduced to 15 °C at a rate of 0.5 °C/min. Those oscillatory settings were verified to be in the linear viscoelastic region as the wax begins to crystallize. The data points of $G'$ and $G''$ were collected during the cooling phase. Once at 15 °C, the sample was held for 30 min before running an oscillatory ramp test (controlled torque between 0.1 and 4000 $\mu$N·m at 0.5 Hz) to measure the yield stress of the gelled network. The yielding point was taken as stress at the $G'$ prior to its sudden drop, signifying that the network had yielded. Measurements were repeated several times to provide reasonable statistical confidence.

**Thermal Properties.** The wax appearance temperature (WAT) and wax precipitation curve (WPC) of the test fluids were measured by differential scanning calorimetry (DSC, 8000-PerkinElmer). Samples were prepared as previously described and left to age for 1 h at 60 °C. The waxy solution ($22 \pm 4$ mg) was fast loaded using a pipet into a 60 $\mu$L stainless steel O-ring sealed DSC pan (PerkinElmer, part number 03190218). Those pans were used as they can tolerate high thermal expansion and prevent solvent loss. With the sample pan loaded, the sample was heated to 60 °C at 5 °C/min and held isothermally for 10 min to remove any sample thermal history and to ensure complete dissolution of $nC_{28}$. The sample was then slowly cooled from 60 to −20 °C at a rate of 5 °C/min. The WAT was taken to be the temperature at the onset of the exothermic transition. The method to determine the WPC is discussed with the data.

**Structural Properties.** PXRD patterns were collected using a Bruker D8 X-ray diffractometer fitted with a LynxEye detector and a Cu K$\alpha$ (1.54 Å) radiation source operating at 40 kV and 40 mA, which was calibrated to a Si standard. To prepare a sample, 20 mL of the waxy solution, without or with asphaltenes, was pipetted into a 40 mL centrifuge tube (Fisher Scientific). The centrifuge tube was then placed in a Peltier concentric cylinder of the rheometer and immersed in water. The sample was heated to 80 °C, held at that temperature for 5 min, lowered to 35 °C at a rate of 10 °C/min before stabilizing for a further 5 min, and then cooled to 15 °C at 0.5 °C/min. The protocol followed that of the rheometer method so that between the two measurements, the sample history was comparable. With the gel formed, the sample was centrifuged (Heraeus Megafuge 16R, Thermo Scientific) at 11,000 rpm for 1 h at 15 °C. The supernatant was removed, and the centrifuged waxy gel was left to dry in a fume hood

for 24 h. The dried waxy deposit was then sampled and ground to a powder using a pestle and mortar so that 0.5 g of sample could be loaded into the Bruker sample holder and pressed gently to form a "flat" sample. Each sample was scanned between $2\theta$ angles from 2 to 50° with a step size of 0.016° at 0.38 s/step. The data were then processed using the HighScore$^+$ software (Malvern Panalytical).

The waxy gel network structure was observed by using an optical microscope (SZX10, Olympus). Following the same sample preparation method, 0.5 mL of the sample was pipetted into a rectangular glass cuvette (length, 4 cm; width, 1 cm: and thickness 3 mm, Spectronic Camspec Ltd.). The glass cuvette was mounted on a temperature-controlled stage (Linkam CAP500) and heated to 80 °C, held for 5 min, and then cooled to 15 °C at 5 °C/min. The sample was held at a constant temperature for 30 min, and the gel network was imaged using the dark field mode of the microscope with 1.6× magnification.

**Polythermal Tests.** Wax crystallization and dissolution temperatures of 100 g/L $nC_{28}$ in 6:4 DodecTol solutions without and with 0.1 g/L RA or IAA were measured using Crystal16 (Technobis Crystallization Systems). One milliliter of the solution was pipetted into 4 × 1.5 mL glass vails and loaded into the thermally controlled cells of the Crystal16. The test fluids were continuously stirred, heated to 40 °C, and held for 15 min to ensure complete dissolution of the wax. Then the temperature was cooled to −10 °C at a specified rate and held for 15 min before being heated to 40 °C at the same rate. Consecutive cooling and heating cycles were run at different rates of 0.2, 0.5, 1, 2, and 3 °C/min. All measurements were repeated at least three times with the mean and standard deviation values for both the crystallization and dissolution temperatures reported.

**Atomic Force Microscopy (AFM).** Following the method of Qiao et al.,[22] adhesion forces between asphaltene subfractions in 6:4 DodecTol were measured using an AFM (MultiMode, Bruker). To prepare the test surfaces, 1 cm² silica wafer substrates (University Wafers, USA) were cleaned by sonicating in 2 wt % Decon for 30 min followed by rinsing with pure DI water, dried with nitrogen gas, and exposed to UV/ozone (ProCleaner, BioForce Nanosciences, USA) for 30 min to remove any residual organics. To coat the surfaces with either RA or IAA, test substrates were submerged in asphaltene (RA or IAA) solutions of 0.05 g/L in toluene for 1 h. The substrates were then removed and gently rinsed with toluene to remove any loosely bound asphaltenes before drying in a fume hood.

Tipless cantilevers (NP-O10, Bruker Scientific, USA, spring constant ∼0.35 N/m) were cleaned by UV/ozone exposure for 30 min prior to mounting the colloidal probes. Silica microspheres ($D \approx$ 10 $\pm$ 2 $\mu$m, Whitehouse Scientific) were soaked in 0.05 g/L asphaltenes (RA or IAA) in toluene for 1 h. Then, three to four drops of the dilute dispersion were deposited on a clean glass slide for the solvent to evaporate. Particles were isolated and carefully mounted at the apex of the tipless AFM silicon nitride cantilevers (NP-O10, Bruker Scientific, USA) by using a two-component epoxy (EP2LV, Master Bon, USA). Images of the prepared probes are provided in the Supporting Information (Figure S2). Prior to measuring the interaction forces, the test cell was filled with 6:4 DodecTol, and the system was allowed to equilibrate for 10 min. Interaction forces were measured using an approach and retraction velocity of 1 $\mu$m/s with no hold time on contact. Two surface locations were chosen to provide a representative measure of the adhesion on surfaces that are heterogeneously contaminated.

## ■ RESULTS AND DISCUSSION

When a waxy fluid is cooled, wax crystals nucleate and grow once the temperature is below the WAT. With the number and size of wax crystals increasing, the wax crystals start interacting and eventually form a contiguous network that is no longer purely viscous but exhibits elasticity. To understand the effect of impurities/additives on this process, it is often appropriate to determine the wax gelation temperature, $T_g$, when $G' = 1$ Pa[16] (Figure 1a). With continued cooling, the elasticity of the
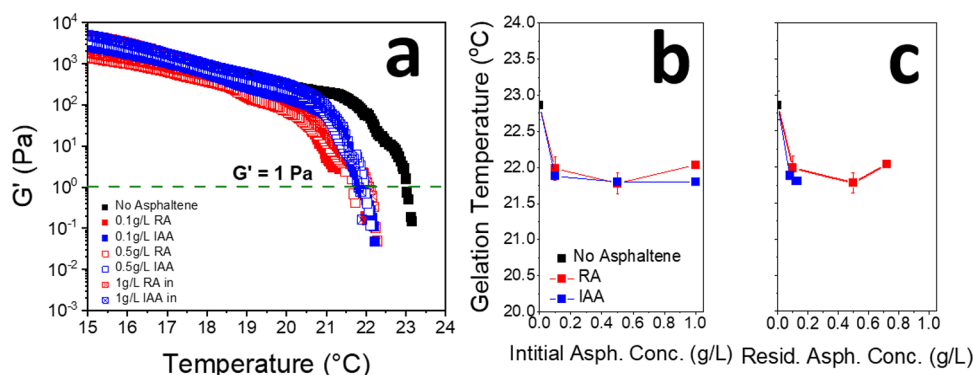
**Figure 1.** Effect of asphaltene concentration on the $T_g$ of 100 g/L $nC_{28}$ waxy fluid in 6:4 DodecTol. Samples were cooled from 40 to 15 °C at 0.5 °C/min. (a) Waxy fluid storage modulus ($G'$) as a function of temperature; (b) $T_g$ as a function of the initial asphaltene concentration (RA: red symbols, IAA: blue symbols); and (c) $T_g$ as a function of the residual asphaltene concentration. The lines are added to guide the eye.

network increases as the system becomes dominated by interactions between the wax crystals.

Figure 1b shows the measured $T_g$ of the waxy solutions prepared to 100 g/L $nC_{28}$ in 6:4 DodecTol with increasing concentrations of RA and IAA. When adding 0.1 g/L asphaltenes, the $T_g$ decreased by 0.9 and 1 °C for RA and IAA, respectively. However, increasing the asphaltene concentration further had a negligible effect on $T_g$, which agrees with Xue et al.[18] who showed that the greatest effect of asphaltenes on $T_g$ is seen at concentrations as low as 0.01 wt % (~0.1 g/L). Furthermore, it is noted that the two asphaltene fractions behaved similarly when lowering the $T_g$; hence, the differences between the asphaltenes, in terms of their chemistry and structure, appears to be negligible when varying $T_g$.

It is worth noting that the IAA fraction is significantly more unstable (i.e., strongly aggregates to form large clusters) than the RA fraction. Hence, during the measurement, IAA will precipitate more, which means that it is more likely to be noninteracting with the waxy solution (Figure S3 in the Supporting Information for the relative stability of the two asphaltene subfractions). To approximate the residual asphaltene concentration (i.e., the amount of nonsedimented asphaltenes), solutions were measured using UV−vis (at 600 and 800 nm) before and after sample aging following the same conditions as the $T_g$ measurement (Figures S4 and S5 of the Supporting Information). When correcting for the residual concentration, it is shown that the observed changes in $T_g$ occur within a similar asphaltene concentration range, i.e. 1 °C drop in $T_g$ when adding 0.1 g/L RA or 0.08 g/L IAA (Figure 1c). However, whereas the effect can be studied up to ~0.8 g/L for RA, the instability of IAA meant that concentrations in excess of ~0.15 g/L could not be studied.

The WAT of the waxy solutions without and with asphaltenes was also measured and found to slightly reduce when either RA or IAA were added to the waxy solution (Table 1). However, the difference with the asphaltene type was considered negligible. The trends are consistent with those seen for $T_g$ (Figure 1) and confirm that the waxy solutions are further subcooled (more supersaturated) when asphaltenes are added, indicating that asphaltenes contribute to a greater barrier to wax crystallizability. These findings contradict those of Li et al.[28] who showed that, when adding asphaltenes to a model waxy oil, the WAT increased, with the increase more significant for the most polar asphaltenes. However, it is worth noting that the four asphaltene fractions considered in that study showed little difference in elemental compositions, i.e.,

**Table 1. WAT of Waxy Solutions (100 g/L $nC_{28}$ in 6:4 DodecTol) Measured without and with RA and IAA[a]**

| asph. type | initial conc. (g/L) | residual conc. (g/L) | WAT (°C) | WAT stan-dev (°C) |
|---|---|---|---|---|
| $nC_{28}$ | 0 | 0 | 27.9 | 0.091 |
| RA | 0.1 | 0.10 | 26.8 | 0.495 |
| RA | 1 | 0.72 | 26.3 | 0.530 |
| IAA | 0.1 | 0.08 | 27.2 | 0.405 |
| IAA | 1 | 0.13 | 26.1 | 0.208 |

[a]Waxy solutions were cooled from 60 to −20 °C at a rate of 5 °C/min.

less than 0.07 wt % difference, unlike in the current study where IAA has O and S contents of 3.39 and 4.03 wt % compared to RA having O and S contents of 2.56 and 3.40 wt %. These differences are more contrasting to assess the effects of asphaltene polarity and point to the performance of the fractionation method being able to separate the most polar asphaltenes from the whole asphaltenes.

Once the waxy solution cooled to 15 °C, it was then possible to measure the yield stress by conducting an oscillatory torque ramp measurement (Figure 2a). The yield stress values as a function of the asphaltene type and concentration are shown in Figure 2b,c for the initial and residual concentrations.

For RA, increasing the asphaltene concentration reduced the yield stress of the waxy gel. Such behavior is consistent with many published studies where authors have attributed the lower yield stress to changes in the wax crystal morphology and size caused by a mutual interaction between asphaltenes and wax molecules,[11,12,20,29] i.e., the interaction between aliphatic chains of asphaltenes and the alkane, or from asphaltene flocs acting as nucleation sites for wax crystal growth. For the former, Li et al.[20] separated asphaltenes into subfractions of varying polarity using an antisolvent method, noting that all asphaltenes reduce the yield stress but that the effect was more significant when adding the least polar (more aliphatic) asphaltene fraction, which the authors stated preferentially interacted with the alkanes. The more aliphatic asphaltenes become incorporated into the wax crystal structure as a coprecipitant, disrupting crystal growth and altering the morphology of the wax crystal from needle-like to globular-like. These changes reduce the extent of entanglement of wax crystals and decrease the amount of wax precipitated. For the latter, Lei et al.[15] suggested that wax molecules crystallize more easily on aggregated asphaltenes that act as nucleation sites,
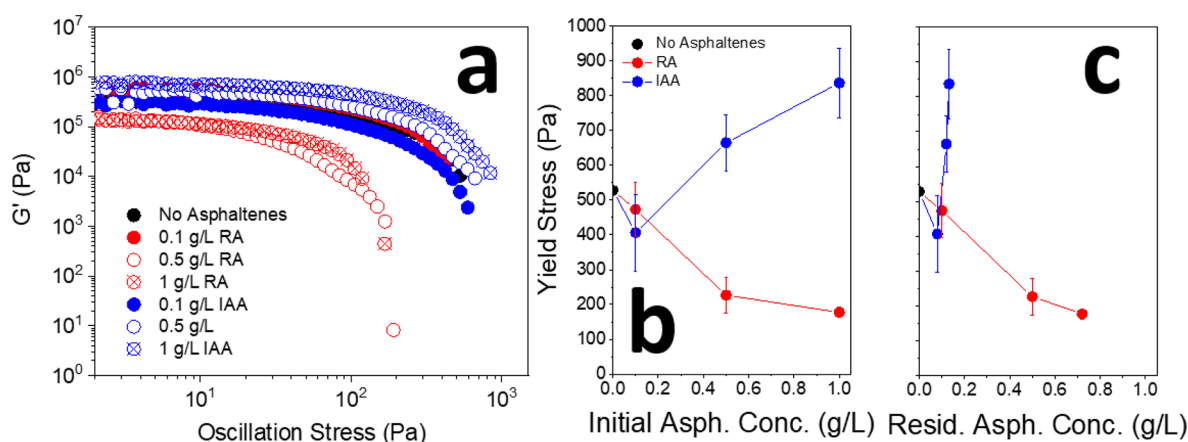
**Figure 2.** Effect of asphaltene concentration on the yield stress of 100 g/L $nC_{28}$ waxy solution in 6:4 DodecTol measured at 15 °C. (a) Waxy fluid storage modulus ($G'$) as a function of oscillatory torque; (b) yield stress as a function of the initial asphaltene concentration (RA: red symbols, IAA: blue symbols); and (c) yield stress as a function of the residual asphaltene concentration. The lines are added to guide the eye.

forming an amorphous wax–asphaltene structure of lower yield stress.

For IAA, the general trend is that the yield stress increases with increasing asphaltene concentration. Considering the initial concentration (Figure 2b), the sample with 0.1 g/L IAA is within error of the waxy solution without asphaltenes; hence, the effect is negligible. But for higher concentrations, the yield stress is seen to increase by ~300 Pa, which is significant and opposite to that observed with RA. When assessed against the residual concentration, this increase in yield stress is found to occur within a small concentration range, ~0.08 to ~0.15 g/L, with the upper concentration being limited by the instability of the IAA fraction.

Ruwoldt et al.[19] studied the effect of asphaltene subfractions on the yield stress of waxy solutions. The behavior for the RA-like fraction is consistent with the current study, but for the IAA-like fraction (i.e., the most polar asphaltenes), which the authors termed "irreversibly adsorbed asphaltenes", the yield stress was slightly reduced, although it was within error of the yield stress without asphaltenes. Although the yield stress was not found to increase, the difference between the current findings and those previously reported may be due to differences in the asphaltene chemistry. For example, Figure 2 shows the contrasting behavior between the RA and IAA fractions, and it appears that the IAA fraction used in the current study is more polar than that extracted by Ruwoldt et al.,[19] suggesting that asphaltene polarity can affect the yield stress of a gelled waxy network.

With yield stress governed by the number and strength of contacts, it is important to first understand if the changes in WAT affect the amount of wax precipitated at 15 °C. This was estimated from the exothermic thermograms as the waxy solutions without and with asphaltenes were cooled from 60 to −20 °C, taking −20 °C as the condition for complete wax crystallization. The wax precipitation curve (WPC) is constructed by measuring the exothermic energy from the onset of crystallization to the reference temperature and normalizing that energy to the full energy of crystallization (Figure 3). At 15 °C, the amount of precipitated wax was 91 g/L without asphaltenes, 90.5 g/L with RA, and 91.2 g/L with IAA. Hence, the difference is negligible and thus would not affect the yield stress as seen in Figure 2. Therefore, such changes in yield stress are likely to be more influenced by the
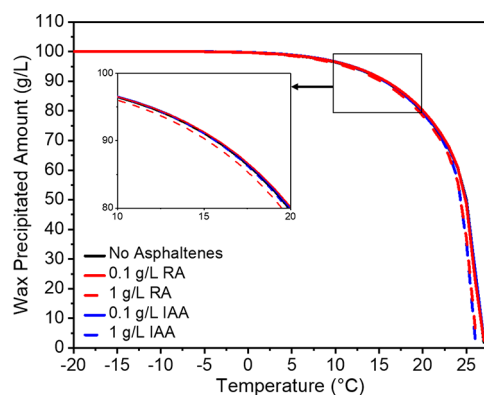


**Figure 3.** Wax precipitation curve of 100 g/L $nC_{28}$ in 6:4 DodecTol without and with RA or IAA added at 0.1 and 1 g/L.

characteristics of the wax crystals (crystal structure, shape, and size) and associated interactions that may be disrupted or promoted by the presence of asphaltenes.

Following crystallization, the lattice structure of $nC_{28}$ was determined to be monoclinic ($p$XRD pattern in Figure S6) as identified by the International Centre for Diffraction Data (ICDD).[30] When adding either RA or IAA to the waxy solutions, the lattice structure remained consistent, and so the presence of asphaltenes did not modify the crystal unit cell.

Although the lattice remains monoclinic, lattice strain caused by disruption to the interlamellar structure ($c$-axis direction) can affect the mechanical properties of the solid wax.[18,31,32] The degree of structural disorder from the lattice strain along the (0 0 $l$) planes can be assessed using the Williamson and Hall (W−H) method.[31] Using the HighScore+ (Malvern Panalytical) software, each sample was analyzed for the peak shapes of the (0 0 4), (0 0 6), (0 0 8), and (0 0 10) reflections shown in Figure 4. Prior to the analysis, the broadening of the $p$XRD peaks was subtracted from the instrumental broadening, which was determined from a standard silicon sample. The peaks were fitted using a pseudo-Voight function, and the Gaussian integral breadth ($\beta_s$) (eq 1) was determined. It is assumed that the broadening due to particle size is Lorentzian, which is not considered here, and the broadening due to lattice strain is Gaussian:[33]
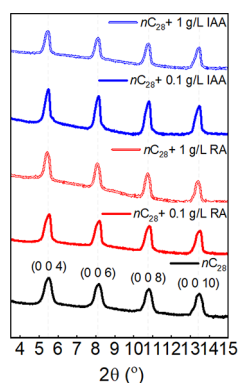
**Figure 4.** pXRD reflections from 4 to 15° for $nC_{28}$ wax crystals with RA and IAA added at 0.1 and 1 g/L. The wax crystals were formed by cooling 100 g/L $nC_{28}$ at 0.5 °C/min from 40 to 15 °C in 6:4 DodecTol.

$$\beta_S \cos\theta = [4\varepsilon_{strain} \times \sin\theta] + \frac{K\lambda}{L} \qquad (1)$$

where $\theta$ is the Bragg angle, $\varepsilon_{strain}$ is the mean strain, $L$ is the mean crystallite size, $\lambda$ is the radiation wavelength taken as 1.5406 Å, and $K$ is the shape factor that for spherical particles is 0.90.

For the pure $nC_{28}$ sample, the slope of $\beta_S \cos\theta$ against $\sin\theta$ is negligible, confirming a strain-free crystal lattice. All slopes increased when adding RA or IAA (Figure 5a), confirming the lattice is strained in the range of 0.2% (0.1 g/L RA) to 0.37% (0.1 g/L IAA) (see Figure 5b). The increased strain is also seen from the peak broadening of the (0 0 4), (0 0 6), (0 0 8), and (0 0 10) reflections (Figure S7 of the Supporting Information), verifying that asphaltenes can be incorporated into the wax lamellar structure. For RA, the lattice strain increases with higher asphaltene concentration, and this may be the reason for the reduced yield strength of the waxy gel. The effect may be similar to that described by Xue et al.[18] who noted an increase in the c-axis of the crystal lattice when adding asphaltenes, which the authors attributed to a greater conformational disorder (caused by chain end-gauche effects) and a weaker gel structure. However, a similar lattice strain is also induced by the IAA fraction, but the yield stress of the waxy fluid generally increases with higher asphaltene content (Figure 2c). This contradiction between the asphaltenes subfractions likely suggests that the asphaltenes (RA or IAA)

act differently within the waxy lamellar structure, particularly the IAA fraction as a yield stress increase with asphaltenes has not been reported.

Dark field (DF) microscopy images were collected to evaluate if the gel network structure is modified by the two asphaltene subfractions (RA and IAA). Without asphaltenes (100 g/L $nC_{28}$ in 6:4 DodecTol), the wax crystals appear needle-like (Figure 6a) and do not show any preferred alignment. The random orientation leads to significant interlocking of the needlelike crystals, which generates the yield stress, with substantial crystal breakage having to occur so the material can flow. With adding 0.1 g/L RA (Figure 6b), the wax crystals remain needle-like; however, a significant fraction of the image shows discrete patches with diffuse features. When observed under higher magnification (Figure 6b inset), those discrete patches are found to be composed of shorter and thinner needle-like crystals branching out from a common center, and at higher asphaltene concentrations, those discrete patches become even more prominent (Figure 6c). Although those patches can be seen in the IAA sample, they are only visible at the highest asphaltene concentration (1 g/L IAA, Figure 6e), but the discrete patches are fewer and smaller than those observed in the RA sample. The 0.1 g/L IAA sample (Figure 6d) resembles the structure without asphaltenes, which may confirm why the two yield stresses are similar (Figure 2).

Those discrete patches likely indicate differences in the nucleation mechanism, which can be described by instantaneous and progressive nucleation. The former describes a process in which all crystal nuclei appear simultaneously followed by crystal growth, whereas the latter describes a progressive process wherein nucleation sites have different activation energies, which lead to the continuous generation of new nuclei among already growing crystals. This mechanism produces crystals with a greater polydispersity.[34]

To determine the crystallization mechanism, the Kashchiev−Borissova−Hammond−Roberts (KBHR)[35,36] method was followed. The method relates the relative critical undercooling ($u_c$) to the cooling rate ($q$). The slopes from a fitted linear regression of $\ln u_c$ vs $\ln q$ provides information as to the dominant nucleation mechanism. A slope >3 indicates progressive nucleation, whereas a slope <3 is instantaneous nucleation. A comprehensive description of the KBHR method can be found in Camacho et al.[37] The polythermals and $\ln u_c$ vs $\ln q$ plots used for determining the nucleation mechanisms
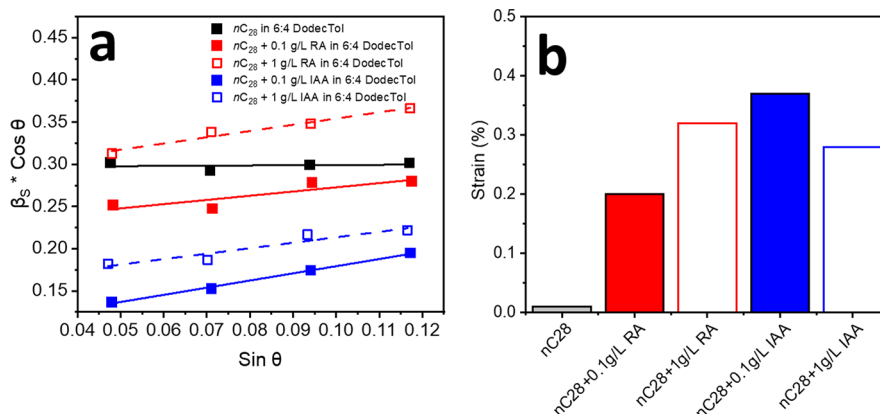


**Figure 5.** (a) Williamson and Hall plots of n-Octacosane powders formed by cooling 100 g/L of $nC_{28}$ in 6:4 DodecTol at 0.5 °C/min to 15 °C in the absence and presence of RA or IAA at 0.1 and 1g/L. (b) Lattice strain with and without RA or IAA at 0.1 and 1g/L.
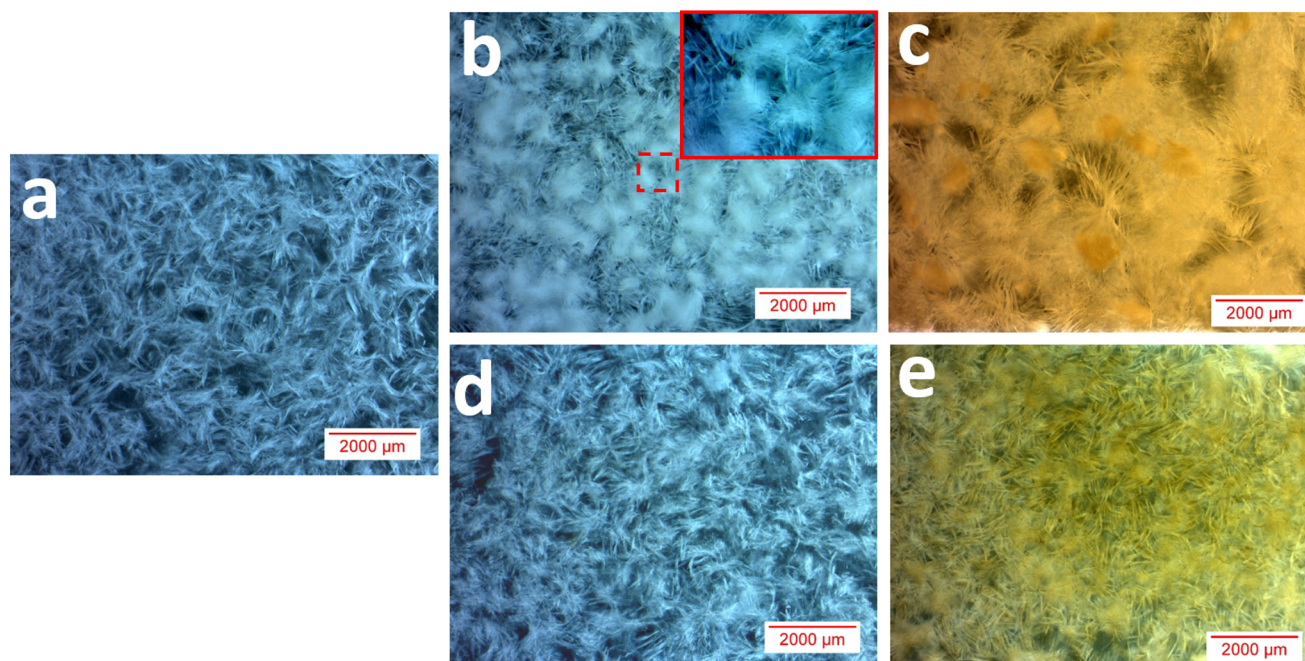
**Figure 6.** Dark field micrographs of waxy gels formed by cooling 100 g/L $nC_{28}$ in 6:4 DodecTol at 0.5 °C/min to 15 °C from 80 °C without asphaltenes (a) and with RA (b and c) or IAA (d and e) at 0.1 g/L asphaltenes (b and d) and 1 g/L asphaltenes (c and e). Concentrations refer to the prepared concentration.

**Table 2. Nucleation Mechanisms Determined from $u_c$ vs $q$ slopes in ln−ln coordinates (Figure S9) for $nC_{28}$ in 6:4 DodecTol with No Asphaltenes, RA, or IAA**

| asp. type | $nC_{28}$ concentration (g/L) | asph. concentration (g/L) | slope | $R^2$ | nucleation mechanism |
|---|---|---|---|---|---|
| no asphaltene | 100 | 0 | 3.48 | 0.94 | PN |
| RA | 100 | 0.1 | 5.57 | 0.98 | PN |
| IAA | 100 | 0.1 | 3.16 | 0.93 | PN |

of 100 g/L $nC_{28}$ in DodecTol without and with RA or IAA are shown in Figures S8 and S9 in the Supporting Information.

Because the method relies on light transmission, only samples of pure wax and those with 0.1 g/L asphaltenes could be accurately measured. Progressive nucleation is found to be the dominant mechanism in all samples (Table 2), although the 0.1 g/L RA is significantly more progressive (slope = 5.57) than the other two samples, which are similar. These findings are in good agreement with the observations in Figure 6 and confirm that those discrete patches are formed as a result the more progressive nucleation, which leads to the greater polydispersity of the wax crystals. More progressive nucleation has been shown to occur when adding small molecular additives that change the nucleation pathway from instantaneous to progressive. These additives bind to the solute, which inhibit the formation of uniform and stable prenucleation clusters.[38,39] Although not considered here, it is thought that the asphaltenes can have a similar effect, which may suggest that the RA fraction interacts with the n-octacosane to disrupt the formation of stable n-octacosane prenuclei but less so the IAA fraction. Previous studies have shown that asphaltenes that are more paraffinic (less aromatic and less polar) can be better incorporated into the wax crystal structure.[10,20] Of the two subfractions, the RA fraction is less polar, is more aromatic, and forms smaller nanoaggregates/clusters than the IAA fraction; hence, it would not necessarily agree with those previous findings. However, those studies used less aliphatic solvents than the current study, and so those asphaltenes

would be better dispersed than the asphaltenes in the current study. Of the two fractions, RA and IAA, RA are more dispersible (only molecules and nanoaggregates in good solvents) than IAA and so may be more preferable to interact with the wax crystals, similar to those previous findings.

Although it may be possible for asphaltenes to act as nucleation sites for wax crystals,[13] the inconsistency in behavior between the RA and IAA samples and the lower WAT (Table 1) rather than a higher WAT likely indicate that this is not the case in the current study. With more progressive nucleation, more diffuse patches are formed, and although not discussed in regard to the nucleation mechanism, these patches are likely similar to those previously observed by Venkatesan et al.,[10] who described a transition from needle-like to globule-like crystals when adding asphaltenes. Our study shows that these globular structures are not due to a change in crystal shape but clusters of smaller needle-like wax crystals that are formed because of the highly progressive nucleation environment. These structures that are frequently seen as globule-like crystals correlate to the drop in yield stress due to less entanglement[9] and the creation of weaker interfloc links within the gel network.[18] This may be the case and would support our current observations for the RA sample, but it is clear that the effect cannot describe the yield stress increase of the IAA sample.

With both asphaltenes being partially incorporated into the waxy gel structure and coating the wax crystals, the contrasting yield stresses could result from differences between interacting

IAA—IAA and RA—RA. It has been suggested by Ruwoldt et al.[19] that asphaltenes can act as "connectors" to maintain a high yield strength, but the ability to "connect" and provide network strength has not been verified. Here we have taken the two asphaltene fractions (RA and IAA) and measured the adhesion forces between two like surfaces, i.e., RA—RA and IAA—IAA (see Figure S10 of the Supporting Information for the approach and retract force curves between the two fractions).

Using the colloidal-probe method of AFM, Figure 7a shows the range of adhesion forces measured between the two
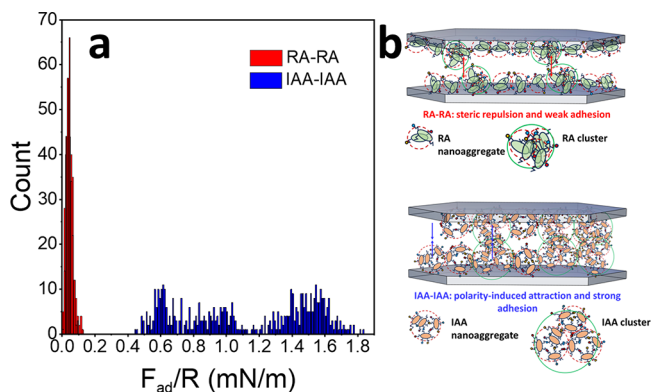


**Figure 7.** Normalized adhesion forces ($F_{ad}/R$) between RA and RA and between IAA and IAA in 6:4 DodecTol. Two different locations on each surface were measured, and 256 force curves were taken at each location (a). The approach and retract force curves are provided in the Supporting Information (Figure S10). Schematic showing interacting RA-coated and IAA-coated wax crystals. The abundance of heteroatoms (N, S, and O) in the IAA fraction promotes the strong attraction between IAA and IAA layers, whereas the RA—RA interaction is repulsive, and so the adhesion force is negligible when the two layers are pushed into contact (b).

asphaltene fractions. For RA, the adhesion forces are very low, less than 0.13 mN/m, with a mean of ∼0.04 mN/m. Meanwhile, for IAA, the adhesion forces are much higher with a mean adhesion force of ∼1.12 mN/m and with greater variation in the measured adhesion forces. With both asphaltenes coating the wax crystals, the contrasting yield stresses of the waxy fluids result from the differences in adhesion forces of the two asphaltene fractions, with the IAA—IAA attraction causing yield stress growth when adding more IAA and the RA—RA repulsion causing yield stress reduction. The strong attraction between IAA and IAA is due to the abundance of heteroatoms in IAA compared to RA (see Table S1 of the Supporting Information for the differences in N, S, and O heteroatom content), with the heteroatoms providing stronger interactions via hydrogen bonding and electrostatic interactions.[40] The IAA fraction has also previously been shown to form larger, more porous asphaltene nanoaggregates/clusters than the RA fraction,[7] with larger clusters also contributing to the stronger adhesion between contacting layers due to increased interdigitation of IAA—IAA compared to RA—RA. A schematic showing the interactions between the wax crystal surfaces coated with RA and IAA is provided in Figure 7b.

With contradictions about how asphaltenes modify the properties of gelled waxy fluids, this study has highlighted the critical role of the asphaltene—asphaltene interaction (nanoaggregates and clusters), which is important when the wax crystals are coated by asphaltenes. The two asphaltene

fractions behaved similarly when considering crystal nucleation and growth, so the difference in bulk behavior seems to be strongly affected by the interactions between asphaltenes. It has previously been discussed that the asphaltene molecule—wax molecule interactions are important, but for the IAA fraction that has a strong tendency to aggregate, even in good solvents,[7] the asphaltene molecule—wax molecule interactions are thought to be negligible. Moreover, when dispersing RA or IAA in 100 g/L $nC_{28}$ waxy solution in 4:6 DodecTol, a more aromatic solvent, the changes in yield stress of the model waxy oils (Figure S11 of the Supporting Information) were found to be similar to those seen in Figure 2, with the yield stress reducing or increasing when adding RA or IAA, respectively. In more aromatic solvents, the RA fraction is better dispersed (molecules and nanoaggregates), but changes in asphaltene cluster or nanoaggregate size, and even the ratio of clusters to nanoaggregates to molecules, seem to have a negligible influence on the observed yield stress trends. Whereas the RA fraction is sensitive to changes in solvent aromaticity, the IAA fraction is less so, and hence, a change from a weakly aliphatic to weakly aromatic solvent is unlikely to significantly change the aggregated state of the asphaltenes.

This study provides new insight into the mechanisms governing yield stress changes of waxy fluids with asphaltenes and directs thinking toward alleviating such high yield stresses by either mitigating asphaltene—asphaltene interactions or removing the IAA fraction from the crude oil.

## ■ CONCLUSIONS

Waxy fluids with asphaltenes have been studied to better understand the effects of asphaltenes on the properties of the fluids, such as the wax appearance temperature, gelation temperature, yield strength, and wax particle size and shape. Few studies have characterized the effects of asphaltenes on waxy fluids, with findings remaining somewhat inconclusive. In the study presented here, asphaltenes were extracted from a heavy crude oil and further fractionated into strongly and weakly interfacially active asphaltenes, creating two asphaltene fractions of differing physicochemical properties.

For the wax appearance and wax gelation temperatures, adding either RA or IAA lowered the critical temperatures by 1 to 2 °C for asphaltene concentrations <1 g/L. However, when held at 15 °C to gel the waxy fluid, the yield strength of the gelled wax decreased with increasing concentration of RA but increased when adding IAA. The result of this contrasting behavior was explored by comparing the two systems in terms of the amount of wax precipitated, crystal structure, and size of the wax particles. Whereas the particle size was smaller in the presence of RA, which is attributed to a more progressive nucleation process, many other properties were unchanged, and so the increasing yield stress could not be explained; see Table 3 for a summary of the induced effects.

Using colloidal probe atomic force microscopy, interaction forces (adhesion) between like asphaltenes (RA—RA and IAA—IAA) were measured. Between RA and RA, the interaction was repulsive with negligible adhesion, which contrasted with the attraction and strong adhesion between IAA and IAA. As such, the yield stress growth when adding IAA can be attributed to the structure-making potential of the IAA—IAA interaction, whereas the yield stress reduction is partly attributed to the structure-breaking potential of the RA—RA interaction. The study highlights the importance of asphaltene—asphaltene interactions modifying the bulk proper-

**Table 3. Effects of Adding Either RA or IAA to Pure $n$C$_{28}$ in 6:4 DodecTol Solutions**

| property | method | $n$C$_{28}$ + RA | $n$C$_{28}$ + IAA |
|---|---|---|---|
| crystal structure | XRD (peak positions) | no effect | no effect |
| crystal lattice strain | {00$l$} line profile analysis | slightly increase | slightly increase |
| crystal size | microscopy | decrease | slightly decrease |
| crystal morphology | microscopy | no effect | no effect |
| nucleation mechanism | turbidimetry | more progressive | no effect |
| WAT | DSC | decrease | decrease |
| gelation temperature | oscillatory rheology | decrease | decrease |
| wax precipitated amount at 15 °C | DSC | no effect | no effect |
| interparticle adhesion | AFM | decrease | increase |
| gel yield strength at 15 °C | oscillatory rheology | decrease | increase |

ties of gelled waxes, something that has not previously been considered.

## ASSOCIATED CONTENT

### Supporting Information

The Supporting Information is available free of charge at https://pubs.acs.org/doi/10.1021/acs.energyfuels.3c02672.

Further details on the physicochemical properties of the asphaltene subfractions, as well as calibration and experimental data that have been discussed in the manuscript (PDF)

## AUTHOR INFORMATION

### Corresponding Author

**David Harbottle** − *School of Chemical and Process Engineering, University of Leeds, Leeds LS2 9JT, United Kingdom;* orcid.org/0000-0002-0169-517X; Email: d.harbottle@leeds.ac.uk

### Authors

**Abdulraouf Ali** − *School of Chemical and Process Engineering, University of Leeds, Leeds LS2 9JT, United Kingdom*

**Ghinwa Yaghy** − *School of Chemical and Process Engineering, University of Leeds, Leeds LS2 9JT, United Kingdom*

**Laksha Parameswaran** − *School of Chemical and Process Engineering, University of Leeds, Leeds LS2 9JT, United Kingdom*

**Chris S. Hodges** − *School of Chemical and Process Engineering, University of Leeds, Leeds LS2 9JT, United Kingdom;* orcid.org/0000-0002-2252-8645

**Thibaut V.J. Charpentier** − *Baker Hughes, Oilfield Services, Liverpool L33 7TQ, United Kingdom*

**Simon D. Connell** − *School of Physics and Astronomy, University of Leeds, Leeds LS2 9JT, United Kingdom;* orcid.org/0000-0003-2500-5724

**Kevin J. Roberts** − *School of Chemical and Process Engineering, University of Leeds, Leeds LS2 9JT, United Kingdom;* orcid.org/0000-0002-1070-7435

Complete contact information is available at:
https://pubs.acs.org/10.1021/acs.energyfuels.3c02672

### Notes

The authors declare no competing financial interest.

## REFERENCES

(1) Huang, Z.; Lee, H. S.; Senra, M.; Scott Fogler, H. A fundamental model of wax deposition in subsea oil pipelines. *AIChE J.* **2011**, *57* (11), 2955−2964.

(2) Huang, Z.; Zheng, S.; Fogler, H. S. *Wax Deposition: Experimental Characterizations, Theoretical Modeling, and Field Practices*; CRC Press, Taylor and Francis Group, Boca Raton, 2015 DOI: 10.1201/b18482.

(3) Coronado, O.; Kak, A. Workflow to Evaluate Wax Deposition Risk Along Subsea Production Systems. In *Offshore Technology Conference*, OnePetro, 2017; Houston, Texas, USA: Vol. *OTC-27855-MS* D041S050R003 DOI: 10.4043/27855-MS.

(4) Mahir, L. H. A.; Vilas Bôas FáVero, C. u.; Ketjuntiwa, T.; Fogler, H. S.; Larson, R. G. Mechanism of wax deposition on cold surfaces: Gelation and deposit aging. *Energy Fuels* **2019**, *33* (5), 3776−3786.

(5) Natarajan, A.; Kuznicki, N.; Harbottle, D.; Masliyah, J.; Zeng, H.; Xu, Z. Understanding mechanisms of asphaltene adsorption from organic solvent on mica. *Langmuir* **2014**, *30* (31), 9370−9377.

(6) Qiao, P.; Harbottle, D.; Tchoukov, P.; Wang, X.; Xu, Z. Asphaltene subfractions responsible for stabilizing water-in-crude oil emulsions. Part 3. effect of solvent aromaticity. *Energy Fuels* **2017**, *31* (9), 9179−9187.

(7) Ballard, D.; Qiao, P.; Cattoz, B.; Dowding, P.; Prevost, S.; Alshamsi, M.; Charpentier, T.; Roberts, K.; Xu, Z.; Harbottle, D. Aggregation Behavior of E-SARA Asphaltene Fractions Studied by Small-Angle Neutron Scattering. *Energy Fuels* **2020**, *34* (6), 6894−6903.

(8) García, M. d. C.; Carbognani, L. Asphaltene− paraffin structural interactions. Effect on crude oil stability. *Energy Fuels* **2001**, *15* (5), 1021−1027.

(9) Fang, L.; Zhang, X.; Ma, J.; Zhang, B. Investigation into a Pour Point Depressant for Shengli Crude Oil. *Ind. Eng. Chem. Res.* **2012**, *51* (36), 11605−11612.

(10) Venkatesan, R.; Östlund, J.-A.; Chawla, H.; Wattana, P.; Nydén, M.; Fogler, H. S. The effect of asphaltenes on the gelation of waxy oils. *Energy Fuels* **2003**, *17* (6), 1630−1640.

(11) Oh, K.; Deo, M. Characteristics of wax gel formation in the presence of asphaltenes. *Energy Fuels* **2009**, *23* (3), 1289−1293.

(12) Alcazar-Vara, L. A.; Buenrostro-Gonzalez, E. Characterization of the wax precipitation in Mexican crude oils. *Fuel Process. Technol.* **2011**, *92* (12), 2366−2374.

(13) Yang, X.; Kilpatrick, P. Asphaltenes and waxes do not interact synergistically and coprecipitate in solid organic deposits. *Energy Fuels* **2005**, *19* (4), 1360−1375.

(14) Kriz, P.; Andersen, S. I. Effect of asphaltenes on crude oil wax crystallization. *Energy Fuels* **2005**, *19* (3), 948−953.

(15) Lei, Y.; Han, S.; Zhang, J.; Bao, Y.; Yao, Z.; Xu, Y. n. Study on the effect of dispersed and aggregated asphaltene on wax crystallization, gelation, and flow behavior of crude oil. *Energy Fuels* **2014**, *28* (4), 2314−2321.

(16) Tinsley, J. F.; Jahnke, J. P.; Dettman, H. D.; Prud'home, R. K. Waxy gels with asphaltenes 1: Characterization of precipitation, gelation, yield stress, and morphology. *Energy Fuels* **2009**, *23* (4), 2056−2064.

(17) Ruwoldt, J.; Simon, S.; Norrman, J.; Oschmann, H.-J. r.; Sjöblom, J. Wax-inhibitor interactions studied by isothermal titration calorimetry and effect of wax inhibitor on wax crystallization. *Energy Fuels* **2017**, *31* (7), 6838−6847.

(18) Xue, H.; Zhang, J.; Han, S.; Sun, M.; Yan, X.; Li, H. Effect of asphaltenes on the structure and surface properties of wax crystals in waxy oils. *Energy Fuels* **2019**, *33* (10), 9570−9584.

(19) Ruwoldt, J.; Subramanian, S.; Simon, S.; Oschmann, H.; Sjöblom, J. Asphaltene fractionation based on adsorption onto calcium carbonate: Part 3. Effect of asphaltenes on wax crystallization. *Colloids Surfaces: Physicochemical Engineering Aspects* **2018**, *554*, 129−141.

(20) Li, Y.; Han, S.; Lu, Y.; Zhang, J. Influence of asphaltene polarity on crystallization and gelation of waxy oils. *Energy Fuels* **2018**, *32* (2), 1491−1497.

(21) Qiao, P.; Harbottle, D.; Tchoukov, P.; Masliyah, J.; Sjoblom, J.; Liu, Q.; Xu, Z. Fractionation of asphaltenes in understanding their role in petroleum emulsion stability and fouling. *Energy Fuels* **2017**, *31* (4), 3330−3337.

(22) Qiao, P.; Harbottle, D.; Li, Z.; Tang, Y.; Xu, Z. Interactions of Asphaltene Subfractions in Organic Media of Varying Aromaticity. *Energy Fuels* **2018**, *32* (10), 10478−10485.

(23) Yang, F.; Tchoukov, P.; Pensini, E.; Dabros, T.; Czarnecki, J.; Masliyah, J.; Xu, Z. Asphaltene subfractions responsible for stabilizing water-in-crude oil emulsions. Part 1: interfacial behaviors. *Energy Fuels* **2014**, *28* (11), 6897−6904.

(24) Ballard, D. A.; Chacón-Patiño, M. L.; Qiao, P.; Roberts, K. J.; Rae, R.; Dowding, P. J.; Xu, Z.; Harbottle, D. Molecular characterization of strongly and weakly interfacially active asphaltenes by high-resolution mass spectrometry. *Energy Fuels* **2020**, *34* (11), 13966−13976.

(25) Zeng, H.; Tessarolo, N.; Gonzalez, D.; Gramin, P.; Wicking, C.; Pietrobon, M. Sticky molecules" on rock surface might play an important role in formation damage due to asphaltene deposition. *Fuel* **2020**, *277*, No. 117983.

(26) Mojica, D.; Angeles, M.; Alvarez, O.; Pradilla, D. Asphaltene Precipitation and the Influence of Dispersants and Inhibitors on Morphology Probed by AFM. *Colloids and Interfaces* **2023**, *7* (1), 3.

(27) Li, W.; Li, H.; Da, H.; Hu, K.; Zhang, Y.; Teng, L. Influence of pour point depressants (PPDs) on wax deposition: A study on wax deposit characteristics and pipeline pigging. *Fuel Process. Technol.* **2021**, *217*, No. 106817.

(28) Li, C.; Zhu, H.; Yang, F.; Liu, H.; Wang, F.; Sun, G.; Yao, B. Effect of asphaltene polarity on wax precipitation and deposition characteristics of waxy oils. *Energy Fuels* **2019**, *33* (8), 7225−7233.

(29) Alcazar-Vara, L. A.; Buenrostro-Gonzalez, E. Experimental study of the influence of solvent and asphaltenes on liquid−solid phase behavior of paraffinic model systems by using DSC and FT-IR techniques. *Journal of Thermal Analysis Calorimetry* **2012**, *107* (3), 1321−1329.

(30) Platonova, N.; Kotelnikova, E.; Filatov, S. St. Petersburg State University; Department of Crystallography, Russian Federation., *ICDD Grant-in-Aid*, 2010.

(31) Craig, S.; Hastie, G.; Roberts, K. Chain length dependent polymorphism in even number n-alkanes: line profile analysis of synchrotron powder X-ray diffraction data. *Journal of Materials Science Letters* **1996**, *15* (14), 1193−1196.

(32) Chevallier, V.; Provost, E.; Bourdet, J.; Bouroukba, M.; Petitjean, D.; Dirand, M. Mixtures of numerous different n-alkanes: 1. Structural studies by X-ray diffraction at room temperature—correlation between the crystallographic long c parameter and the average composition of multi-alkane phases. *J. Polym. Sci.* **1999**, *40* (8), 2121−2128.

(33) Craig, S.; Hastie, G.; Roberts, K.; Gerson, A.; Sherwood, J.; Tack, R. Investigation into the structures of binary-, tertiary-and quinternary-mixtures of n-alkanes and real diesel waxes using high-resolution synchrotron X-ray powder diffraction. *J. Mater. Chem.* **1998**, *8* (4), 859−869.

(34) Corzo, D. M. C.; Borissova, A.; Hammond, R. B.; Kashchiev, D.; Roberts, K. J.; Lewtas, K.; More, I. Nucleation mechanism and kinetics from the analysis of polythermal crystallisation data: methyl stearate from kerosene solutions. *CrystEngComm* **2014**, *16* (6), 974−991.

(35) Kashchiev, D.; Borissova, A.; Hammond, R. B.; Roberts, K. J. Effect of cooling rate on the critical undercooling for crystallization. *J. Cryst. Growth* **2010**, *312* (5), 698−704.

(36) Kashchiev, D.; Borissova, A.; Hammond, R. B.; Roberts, K. J. Dependence of the critical undercooling for crystallization on the cooling rate. *J. Phys. Chem. B* **2010**, *114* (16), 5441−5446.

(37) Camacho, D. M.; Roberts, K. J.; More, I.; Lewtas, K. Solubility and nucleation of methyl stearate as a function of crystallization environment. *Energy Fuels* **2018**, *32* (3), 3447−3459.

(38) Kaskiewicz, P. L.; Downie, R.; Dowding, P. J.; George, N.; Roberts, K. J. Influence of a polymeric additive on the crystallisability and nucleation mechanism for the model fuel system of eicosane crystallising from supersaturated toluene solutions. *J. Cryst. Growth* **2022**, *581*, No. 126470.

(39) Kaskiewicz, P. L.; Rosbottom, I.; Hammond, R. B.; Warren, N. J.; Morton, C.; Dowding, P. J.; George, N.; Roberts, K. J. Understanding and Designing Tailor-Made Additives for Controlling Nucleation: Case Study of p-Aminobenzoic Acid Crystallizing from Ethanolic Solutions. *Cryst. Growth Des.* **2021**, *21* (4), 1946−1958.

(40) Ballard, D.; Pickering, J.; Rosbottom, I.; Tangparitkul, S.; Roberts, K.; Rae, R.; Dowding, P.; Hammond, R.; Harbottle, D. Molecular survey of strongly and weakly interfacially active asphaltenes: an intermolecular force field approach. *Energy Fuels* **2021**, *35* (21), 17424−17433.